Improvement of Performance of Modulation Response and Bandwidth of InAs/GaAs Quantum-Dot Laser Diode

Dr. Thaira Z. Altayyar
Electrical Engineering Department, University of Technology/Baghdad.
Email:dr.tyra.uot@hotmail.com
Dr. Hadi T. Ziboon
Electrical Engineering Department, University of Technology/Baghdad.
Email:haditarishziboon@yhoo.co.ut
Jassim Mohammed Sahan
Engineering College, University of Al-Nahrain /Baghdad.
Email:jasimsahan@gmail.com

Received on: 19/3/2014 & Accepted on:7/3/2015

ABSTRACT

This paper proposes a design model of InAs QD laser diode structure, the dimensions of the proposed model have an active region of length 800 μm, width 12 μm, and a height of 375 nm. The proposed model of QD is disk shaped, its height is 2nm and diameter is 14nm. The QDs surface density per layer is 7×10^{12} cm^{-2}, number of QDs layers are 5 layers, wetting layer thickness is 1nm and barrier thickness is 90nm.

The evaluation of the proposed model is based on rate equations model. The InAs/GaAs QD lasers are capable of working at a very low threshold current, which is very important for the development of optical fiber communication systems. Modulation characteristics of *InAs/GaAs* quantum dot (QD) lasers of 1.3μm wavelength have been carefully studied at various bias currents and *K*-factor, the (-3 dB) bandwidth is improved at first as increasing the injected current, in addition, at large injected current, maximum value of the bandwidth is limited by *K*-factor, and the *K*- factor is mainly determined by the photon lifetime and the effective capture time, the *K*-factor can be minimized by choosing an optimum photon lifetime.

The results show that the QD laser diode has a lower threshold current (2 mA), the threshold current density (20 A/cm^2), bias voltage 0.92 V, while output optical power has the range of (0-25 mW), the slope efficiency is 0.25W/A**.** The highest relaxation oscillation frequency at room temperature is 10.18 GHz, corresponding to a modulation bandwidth of 3 GHz due to the small damping factor. Using these parameters, the maximum modulation bandwidth ($f_{-3dB}max$) is estimated as 15.56 GHz.

Keywords: Quantum dots, laser diode, rate equations, modulation bandwidth.

تحسين أداء استجابة التضمين وعرض الحزمة لدايود ليزر نقط الكم نوع InAs/GaAs

الخلاصة

يقدم هذا البحث مقترحا لتصميم دايود الليزر النقط الكمي من المادة InAs بالأبعاد التالية: طول المنطقة الفعالة (800µm), عرض (12 µm), ارتفاع (375 nm). كثافة النقط الكم (7×10^{12} cm^{-2}) لكل طبقة ,عدد الطبقات (5), ارتفاع الطبقة الرطبة (1 nm) وارتفاع طبقة الاستنزاف (90 nm). اعتمادا على شكل القرص الكمي المقترح لنقطة الكم بالأبعاد التالية: سمك (2 nm) وقطر (14 nm).

ويستند تقييم النموذج المقترح على معادلات معدل ليزر نقط الكم لمادة شبة الموصل InAs/GaAs هي قادرة على العمل في العتبة تيار منخفضة جدا، وهو أمر مهم جدا لتطوير نظم الاتصالات في الألياف البصرية, وان خصائص التضمين ليزر نقطة الكم (QD) للطول الموجي 1.3µm تم دراستها بعناية على مختلف التيارات التحيز وعامل-*K* , وقد تم تحسين عرض النطاق الترددي عند (*-3dB*) في البداية عند زيادة حقن التيار، بالإضافة إلى ذلك، ولوحظ ان في زيادة اكبر للحقن التيار فان الحد الأقصى لقيمة عرض النطاق الترددي محدودة بسبب عامل-*K*، والذي تم تحديد عامل-*K* أساسا من العمر الفوتون وزمن التقاط فعالة، فإن يمكن تقليله من اختيار عمر الفوتون الأمثل. النتائج النظرية للدايود المقترح, كانت تيار العتبة (2 mA), كثافة تيار العتبة, (20 A/cm^2), فولتية الانحياز (0.96 V), مدى القدرة الضوئية المنبعثة (0-25 mW) ضمن نطاق الطول ألموجي (1298-1307 nm), وان كفاءة الميل (0.25 W/A), ومقدار عرض الحزمة الترددية (3GHz)عند التردد الرنين (11.69 GHz). وان أعلى تردد التذبذب في درجة حرارة الغرفة هو (10.18 GHz)، المقابل لعرض النطاق الترددي (3 GHz) بفعل عامل التخميد الصغيرة و باستخدام هذه المعايير، يقدر الحد الأقصى لعرض النطاق الترددي الحد الأقصى(15.56GHz).

INTRODUCTION

Semiconductor nano-particles, often referred as quantum dots [1]. That nanoparticles are zero dimensional, possessing nanometric dimensions in all the three dimensions. The diameters of nanoparticles can vary anywhere between one and a few hundreds of nanometers. Small nanoparticles with diameters of a few nanometers are comparable to molecules. Nanoparticles are of great scientific interest because they exhibit unique electronic, optical and photonic properties [2]. Nanoparticle with exciton Bohr diameter exhibits a blue shift in the exciton energy, which is the so-called quantum size effect. It is explained that the continuous energy band of the bulk crystal transforms into a series of discrete energy states resulting in the broadening of the band gap due to the finite size of the nanoparticle [2]. The quantum dot active layers laser is somewhat better than quantum well (QW). The QW laser is somewhat better than conventional lasers with bulk active layers. One obvious advantage is the ability to vary the lasing wavelength merely by changing the width of the quantum of the QW. A more fundamental advantage is that the QW lasers delivers more gain per injected carrier than conventional lasers, which results in lower threshold currents [3].

The 1.3µm InAs/GaAs quantum dot (QD) lasers are the most promising light sources for future local area networks, due to the predicted high modulation speed, improved temperature performance and low threshold current. Significant advancement has been demonstrated the first room-temperature 1.3µm QD lasers in 1998 [4]. On the other hand, the availability of high speed direct modulation 1.3 µm InAs/GaAs QD lasers is of great interest [4].

As with any other semiconductor light source, also in QD lasers, there are the well-known electronic transitions between conduction band (CB) and valence band (VB).

The model can be divided into two parts, photon equations and electron equations. Thus, QD lasers are modeled with four carrier rate equations: two for GS, ES and the latter is for wetting layer (WL) and SCH barrier layer with one rate equations related to photon populations. The presence of more than one state in the dot, is then, taken into account by including the ES. The inclusion of higher excited states is not so important since its population is neglected ordinarily.

Rate Equations Model

The numerical model of the QD laser holds under the assumption that the active region consists of only one QD ensemble, where QDs are interconnected by a wetting layer (WL). It has been assumed that each QD has only two confined energy states, the GS and the ES. The last one has degeneracy equal to four due to the QD symmetry in the growth plane. The carrier energy levels are schematized in Figure (1). Carrier energy can be classified into four levels as follows [5]:

- The SCH energy level where carriers are injected,
- The WL energy level that acts as a common carrier reservoir,
- The dot energy levels (ES and GS) are coupled to the WL.
-

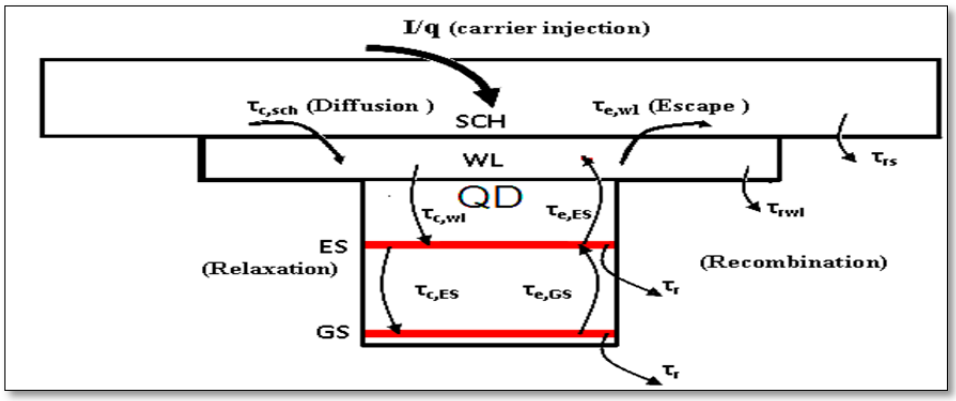

Figure (1) Schematic diagram of the components in the InAs-QD, InGaAs-WL and GaAs-SCH material system of QD-LD for the conduction band energy levels [6].

The carrier dynamics of the initial excitation position and energy level within the barrier towards the QD-GS in Figure (1) as follows [6]:

- Carriers are injected in the SCH barrier at rate I/q, where I is the injection current, q is the elementary charge,
- Relax in the WL state at rate $1/\tau_{c,sch}$ or escape back in the barrier at rate $1/\tau_{e,wl}$,
- From the WL they can be captured in the dot. Therefore, the WL state acts as a common reservoir from which the carriers are captured in the ES at rate $1/\tau_{c,wl}$ and from the ES to the GS at rate $1/\tau_{c,ES}$ where, the times $\tau_{c,sch}$, $\tau_{c,wl}$ and $\tau_{c,ES}$ are the average capture times from the SCH to the WL, from the WL to the ES and from the ES to the GS respectively,
- Carriers escape also from the GS back to the ES at rate $1/\tau_{e,GS}$ or from the ES back to the WL at rate $1/\tau_{e,ES}$ where the emission times $\tau_{e,GS}$ and $\tau_{e,ES}$ are the escape time from the GS back in the ES and the escape from the ES back into the WL,

- Carriers can also recombine with radiative and nonradiative processes from the SCH, the WL and the various confined states with rates l/τ_{rs} , l/τ_{rw} , l/τ_r respectively,

The rate of photons emitted out of the cavity is S_p/τ_p, with τ_p the corresponding photon lifetime of the mode and S_p is the photon occupation probability. It is assumed that the stimulated emission can take place only due to recombination between the electron and hole in the GS [6] The values of all time parameters with description in figure (1) is shown in table (1).

Dot by the rate equations of the occupation probability of the QD states. The resulting REs system for the carrier occupation probability as follows [7]:

$$\frac{dP_{sch}}{dt} = \frac{I}{e} - \frac{P_{sch}(1-P_{wl})}{\tau_{c,sch}} + \frac{P_{wl}}{\tau_{e,wl}} - \frac{P_{sch}}{\tau_{sr}} \quad \dots (1)$$

$$\frac{dP_{wl}}{dt} = \left(\frac{P_{sch}}{\tau_{c,sch}} + \frac{4P_{ES}}{\tau_{e,ES}}\right)(1-P_{wl}) - \frac{P_{wl}}{\tau_{e,wl}} - \frac{P_{wl}}{\tau_{c,wl}}(1-P_{ES}) - \frac{P_{wl}}{\tau_{wr}} \quad \dots . (2)$$

$$\frac{dP_{ES}}{dt} = \left(\frac{P_{wl}}{4\tau_{c,wl}} + \frac{P_{GS}}{2\tau_{e,GS}}\right)(1-P_{ES}) - \frac{P_{ES}}{\tau_{e,ES}}(1-P_{wl}) - \frac{P_{ES}}{\tau_{c,ES}} - \frac{P_{ES}}{\tau_r} \quad \dots (3)$$

$$\frac{dP_{GS}}{dt} = \frac{2P_{ES}(1-P_{GS})}{\tau_{c,ES}} - \frac{P_{GS}(1-P_{ES})}{\tau_{e,GS}} - \frac{P_{GS}}{\tau_r} - \mathrm{v}_g \Gamma \, \mathrm{g}_{GS} \, S_p \quad \dots . (4)$$

$$\frac{dS_p}{dt} = \mathrm{v}_g \Gamma \, \mathrm{g}_{GS} \, S_p - \frac{S_p}{\tau_p} + \beta \frac{2P_{GS}}{\tau_r} \quad \dots (5)$$

Where

P_{ES} and P_{GS} are occupation probabilities of ES, and GS of a QD respectively, and P_{wl} , P_{sch} and S_p the WL and SCH population and the photon occupation respectively.

The occupation probabilities for the GS and ES are defined as follows [8]:

$$P_{GS} = \frac{n_{GS}}{2N_D} \quad \dots (6)$$

$$P_{ES} = \frac{n_{ES}}{4N_D} \quad \dots (7)$$

Where

n_{GS} is the number of electrons in the GS, n_{ES} is the number of electrons in the ES, N_D is the total number of QDs, where P_{wl} , P_{sch} and S_p are the WL and SCH population and the photon occupation respectively and are described by [8];

$$P_{wl} = \frac{n_{wl}}{N_D} \quad \dots (8)$$

$$P_{sch} = \frac{n_{sch}}{N_D} \quad \dots (9)$$

$$S_P = \frac{n_p}{N_D} \quad \dots (10)$$

$$N_D = N_d \, A_o \, N_w \quad \dots (11)$$

$$A_o = L \, W_o \quad \dots (12)$$

where,

n_{sch} is the carrier number in the SCH, n_{wl} is the carrier number in the WL, n_p is the photon number, A_o is the area of QD layer, N_d is the density of the QDs per unit area,

N_w is the number of the QD layers, A is the area of QD layer, W_o is the width of the active layer.

As occupation probabilities approach 1, the relaxation rate decreases, resulting in the occupation of the upper level. Furthermore, at RT and before reaching stimulated emission the system must converge to a quasi-thermal equilibrium characterized by a Fermi distribution of the carriers in all the states. To ensure this convergence the carrier escape times are related to the carrier capture times as follows [6]:

$$\tau_{e,GS} = \tau_{c,ES} \frac{D_{GS}}{D_{ES}} e^{\frac{E_{ES}-E_{GS}}{K_B T}} \quad \ldots (13)$$

$$\tau_{e,ES} = \left(\frac{D_{ES} N_d}{\rho_{wl}}\right) \tau_{c,wl} e^{\frac{E_{wl}-E_{ES}}{K_B T}} \quad \ldots . (14)$$

Where
, the D_{SG} and D_{ES} are the degeneracies of the GS and ES levels respectively. K_B is the Boltzmann constant, and T is the degree of temperature in K^o. The carrier escape time from the ES depends on the ratio between the number of available states in the QDs and in the WL. The E_{GS}, E_{ES} and E_{wl} are the energies of the GS, ES and WL level respectively.
The escape time from the WL to the SCH is as follows [5]:

$$\tau_{e,wl} = \left(\frac{\rho_{wl} N_w}{\rho_{sch} L_{sch}}\right) \tau_{c,sch} e^{\frac{E_{sch}-E_{wl}}{K_B T}} \quad \ldots (15)$$

Where
L_{sch} is the total thickness of the SCH, ρ_{wl} is the DOSs per unit area in the WL and ρ_{sch} is the DOSs per unit volume in SCH, as follows [5]:

$$\rho_{wl} = \frac{m_{ewl} K_B T}{\pi \hbar^2} \quad \ldots (16)$$

$$\rho_{sch} = 2\left(\frac{2\pi m_{esch} K_B T}{\hbar^2}\right)^{\frac{3}{2}} \quad \ldots (17)$$

The steady state solution of the rate equations is obtained by setting all time derivatives to zero. By neglecting, the term $\beta \frac{2P_{GS}}{\tau_r}$ from equation (5) one can get:

$$\frac{1}{\tau_p} = \Gamma v_g g_{GS} \quad \ldots (18)$$

The photon lifetime can be calculated by using equation [9]:

$$\frac{1}{\tau_p} = v_g(\alpha_{int} + \alpha_m) \quad \ldots (19)$$

$$v_g = \frac{c}{\mu_g}$$

where,
α_{int} is the internal loss, α_m is the mirror losses, c is the speed of light in vacuum, μ_g is the material group refractive index.

Output Optical Power

The output optical power (P_{out}) emitted from the front facet of QD-LD is given by [10]:

$$P_{out} = S\ \hbar\omega\ q\ \alpha_m\ v_g\ V \quad \ldots(20)$$

where

S is the photon volume density at steady state, V is the cavity volume, $\hbar\omega$ is the energy per photon, $\hbar$ is a modify of Planck's constant is equal to $h/2\pi$ where, h is Planck's constant.

Structure Design Of Quantum Dot Laser Diode

The nanometer-sized InAs QDs represent localization centers for both electrons and holes since the band gap of *InAs* is lower than that of the surrounding GaAs and InGaAs. The basic structure consists of an active reign comprising QD layer embedded between two cladding layers. The bottom cladding is generally n-doped whereas the top cladding is p-doped. Then by cleaving the device, semiconductor/air interfaces are created to realize mirrors with approximately 30% reflectivity. Electrical confinement is provided by openings in the dielectric cover layer. The volume of the active region V has the form:

$$V = L\ W_O H_O \quad \ldots(21)$$

$$H_o = (L_{sch} + L_{wl} + L_d)N_w \quad \ldots(22)$$

where

L, W_o, and H_o are the length, width and height of active region. This region Contains a five of QD layers, each including a wetting layer (WL), which is typical for samples based on the SK growth method.

The dimensions of the proposed model of the InAs QD laser diode structure and the different layers are:

1. Bottom contact (Ni/AuGe/Au) 0.1μm layer thick, (is connected to the negative electrode of D.C supply) with stripe of 4μm,
2. n-GaAs substrates is grown, all samples (layers) were grown on it,
3. Afterwards a 300nm thick n-GaAs buffer layer,
4. Afterwards a 50nm thick of n-Al GaAs cladding layer.
5. Active region length (L= 800μm), width (W_o= 12μm) and height (H_o= 375nm) with the following contents, as shown in Figure (2):

a. Barrier layer thickness (L_{sch}) as thin GaAs spacer in between the QD layers with thickness of 90nm.

b. InGaAs wetting layer thickness (L_{wl}) is 1nm.

c. The QD is disk shaped with the height (L_d) 2nm and diameter (ρ) 14nm.

d. Number of QDs layers are five layers, and the QDs surface density per layer is 7×10^{12} cm^{-2}.

6. Afterwards a 50nm thick of p-AlGaAs cladding layer,
7. p- GaAs cap layer 60nm thick,
8. SiO_2 insulating layer is 0.1μm thick,
9. Top contact of (Ti/Pt/Au) with thickness of 0.1μm is connected to the positive electrode of D.C supply,
10. Total width (W) is 100μm and length (L) is 800μm for the QD-LD.

This of DQ-LD structure is shown in the Figure (3). Material parameters of InAs-QD, InGaAs-WL and GaAs-SCH layer of the material system as constant parameters are shown in Table (1). Suggested design parameters for the QD-LD are shown in Table (2).

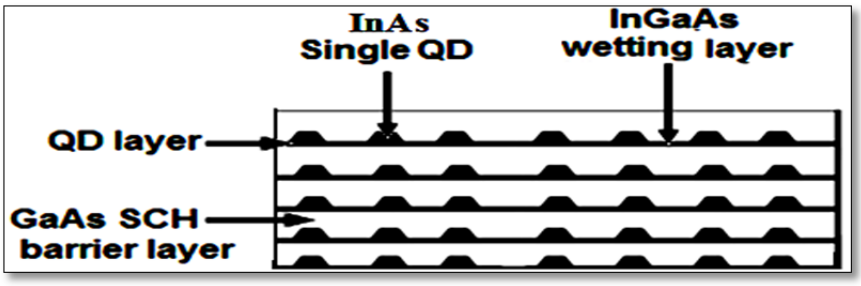

Figure (2) Schematic diagram of the active region cross-sectional view for QD laser diode.

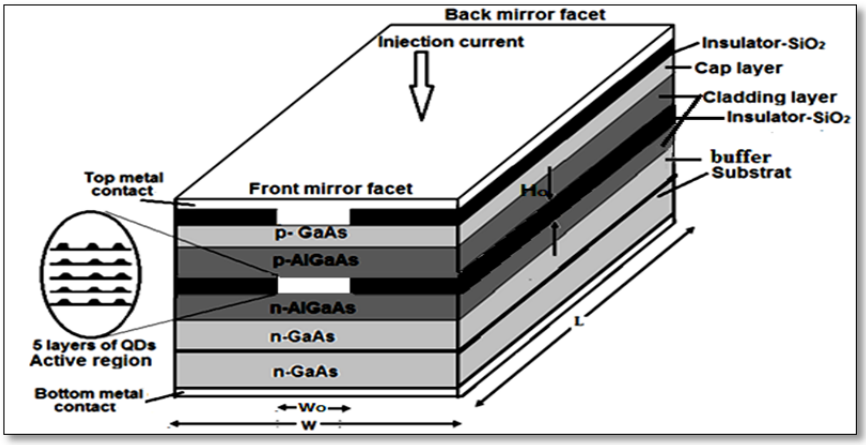

Figure (3) Schematic illustration of the QD-LD structure.

Table (1) Material parameters of InAs-QD, InGaAs-WL and GaAs-SCH material system [5] and [11].

Material parameters	Symbol	Value	Units
ES and GS recombination time	τ_r	*2.8*	*ns*
SCH recombination time	τ_{sr}	*4.5*	*ns*
WL recombination time	τ_{wr}	*3*	*ns*
Capture time from WL to ES	$\tau_{c,wl}$	*1*	*ps*
Capture time from ES to GS	$\tau_{c,ES}$	*7*	*ps*
Diffusion time in SCH	$\tau_{c,sch}$	*6*	*ps*
Energy separation (SCH and WL) state	$E_{SCH\text{-}Wl}$	*84*	*meV*
Average Energy separation (WL and ES)	$E_{Wl\text{-}ES}$	*100*	*meV*
Average Energy separation (ES and GS)	$E_{ES\text{-}GS}$	*80*	*meV*
Free electron mass	m_o	$9.11*10^{-31}$	*Kg*
InAs-QD electron effective mass	m_e	$0.065m_o$	*Kg*
InAs-QD heavy holes effective mass	m_{hh}	$0.377m_o$	*Kg*
InAs-QD refractive index	μ_{QD}	*3.52*	-
GaAs-SCH refractive index	μ_{sch}	*3.65*	-
InGaA- WL refractive index	μ_{wl}	*3.53*	-
Degeneracies of GS and ES, respectively	D_{GS}, D_{ES}	*2, 4*	-

Table (2) Suggested design parameters.

Laser parameters	Symbol	Value	Units	Ref.
Active region width	W_o	*12*	*μm*	-
Active region length	L	*800*	*μm*	-
SCH thickness	L_{sch}	*90*	*nm*	-
WL thickness	L_{wl}	*1*	*nm*	-
Height of QD disk shape	h_o	*2*	*nm*	-
Diameter QD disk shape	d_o	*14*	*nm*	-
Number of QD layers	N_w	*5*	-	-
QD surface density per layer	N_d	7×10^{12}	cm^{-2}	-
Front mirror reflectivity	R_f	*30%,*	-	-
Back mirror reflectivity	R_b	*90%*	-	-
Internal loss	α_{int}	*1*	cm^{-1}	[2]
Spontaneous emission factor	β	10^{-4}	-	[2]
Internal efficiency	η_i	*90%*	-	-
Differential gain of GS	a_{GS}	0.1	cm^{-1}	-
Carrier probability at transparency	P_{tr}	0.5	-	-

Power Current Characteristics

The most important laser characterization is the output optical power from the facet of the laser diode as a function of the inject current, where the injection current begins, the carrier is injected into SCH layer, then relaxes into WL then, the carriers relax down the ladder of states in the dot, so that the dot electron and hole ground states is occupied and the laser is emitted when an electron and a hole recombine. When the injection current reaches to its threshold value of 2.92 mA (threshold current density 30.42A/cm^2), the QD laser diode begins emitting optical power. That optical power increases with increasing injected current. The small scaling of the active region and reduced density of states are caused by a reduction in the threshold current density. Another parameter of interest is the slope efficiency of the curve ($\Delta P/\Delta I$) above the threshold current point, this parameter estimates somehow the power efficiency of the device, i.e higher slope efficiencies means a capability to emit more power in response to lower current injection levels, the slope efficiency is approximately (0.25W/A) the P-I curve of a QD laser diode is shown in figure (4), and power vs. current density characteristics is shown in figure (5).

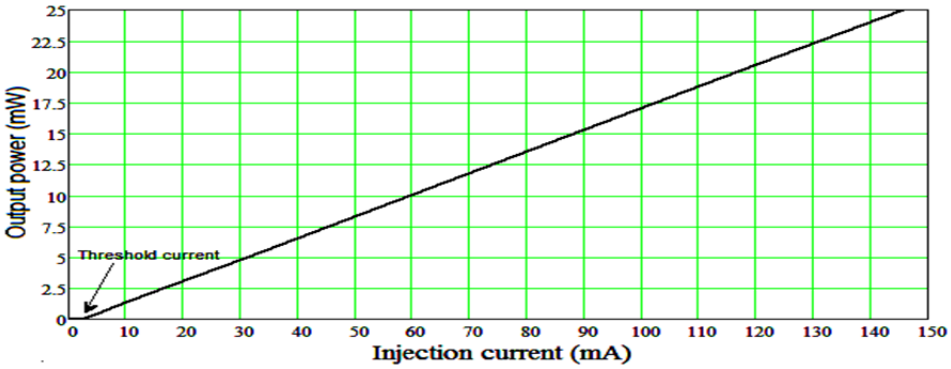

Figure (4) Power vs. current characteristics.

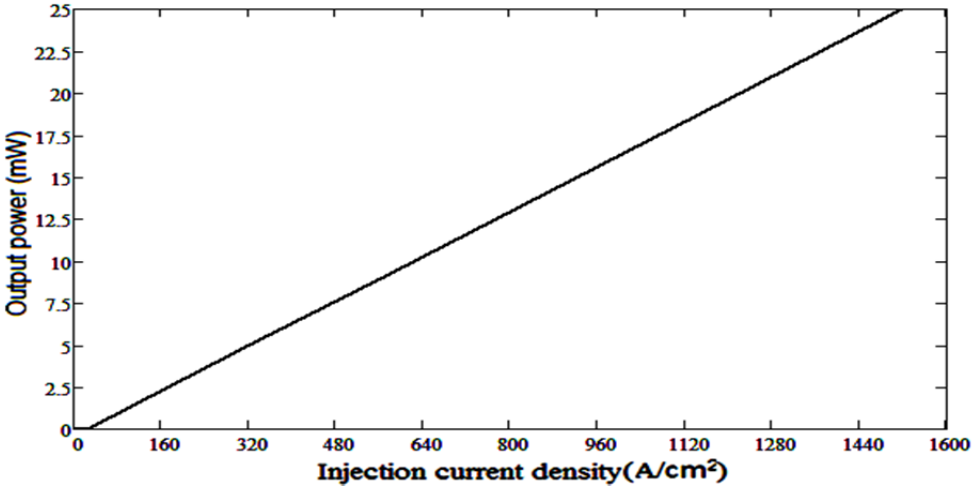

Figure (5) power vs. current density characteristics.

Voltage, Current and Output Power Characteristics

The forward external voltage is applied to the laser diode, where it reaches the threshold bias voltage, the threshold current value is 2.92mA and the laser diode begins operation, then the bias voltage enters a steady state of 0.96V, at that the GS state begins to emit optical output power. The relation of applied biasing voltage and optical output power with respect to injection current is shown in Figure (6).

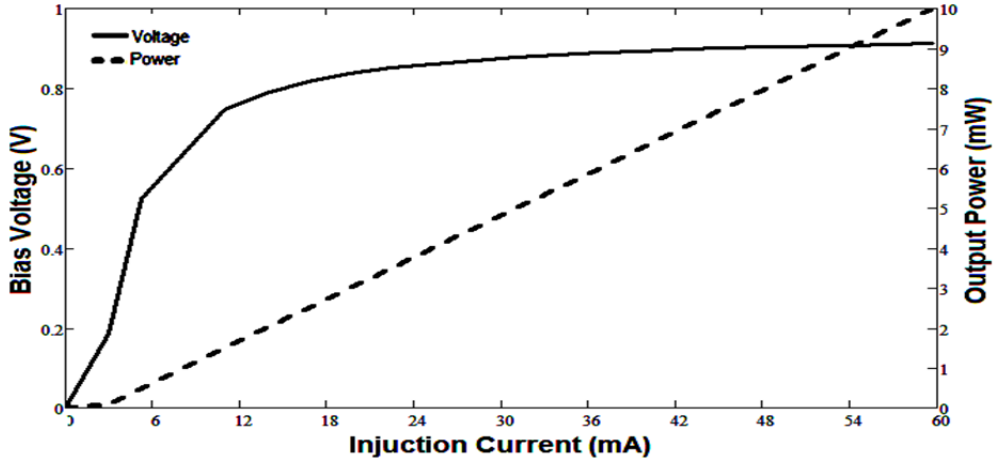

Figure (6) Voltage, current and output power characteristics.

Signal Modulation Response

The direct modulation of a semiconductor laser has been the subject of active research in the area of optical communications. The high modulation bandwidth is a key quantity for the realization of high-speed data communication applications as it limits the maximum possible data rate. Among high-speed properties of QD lasers, K factor and damping factor are two of the most important parameters. The small signal modulation response given by [8]:

$$H(f) = \frac{{f_r}^2}{\left({f_r}^2 - f^2 + j\gamma f/2\pi\right)} \quad \ldots(23)$$

Where

f_r denotes the relaxation oscillation frequency (RO)which is given by [12]:

$$f_r = \frac{1}{2\pi\tau_r}\sqrt{\frac{\tau_r}{\tau_p}\left(\frac{I}{I_{th}} - 1\right)} \quad \ldots(24)$$

Where

, the τ_r is the recombination time and τ_p is the photon lifetime.

The damping factor γ given by [10]:

$$\gamma = \frac{k{f_r}^2}{2\pi} \quad \ldots(25)$$

The relation between γ and f_r is k-factor given by [4]:

$$k = 4\pi^2\left(\tau_p + \tau_{cap}\right) \quad \ldots(26)$$

Where, K is K-factor determines the damping of the modulation response with increasing RO frequency. It is an important parameter in high-speed characteristics of lasers, where τ_{cap} is the capture time between wet layer and lasing state (GS) of QD.

The modulation efficiency (D) of modulation response is given by [9] :

$$D = \frac{f_r}{\sqrt{I - I_{th}}} \quad \ldots(27)$$

At the peak amplitude of modulation is 10dB, relaxation oscillation frequency is 7GHz and bandwidth is 1.6 GHz at injection current 72mA. In our case with K-factor of 57.09 ns, the maximum bandwidth is estimated to be 15.56 GHz with a modulation efficiency of 0.98 GHz /mA$^{1/2}$. The modulation response shown in Figure(7).

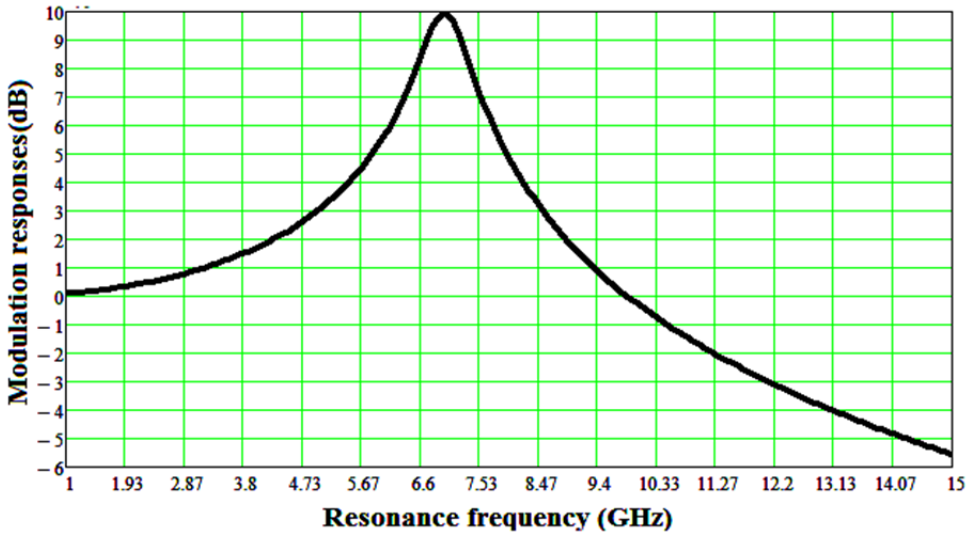

Figure (7) modulation response.

Effect of Injection Current on Modulation Bandwidth

As the static photon density of the GS in the laser diode cavity increases by increasing the injected current, so that the relaxation oscillation frequency increases,

which causes the increase in modulation bandwidth as shown in the figure (8).The dependence of the relaxation oscillation frequency on the square root of current above the threshold of QD. Figure (9) shows a plot of the relaxation oscillation frequency f_r of the modulation response versus the square root of the injection current.

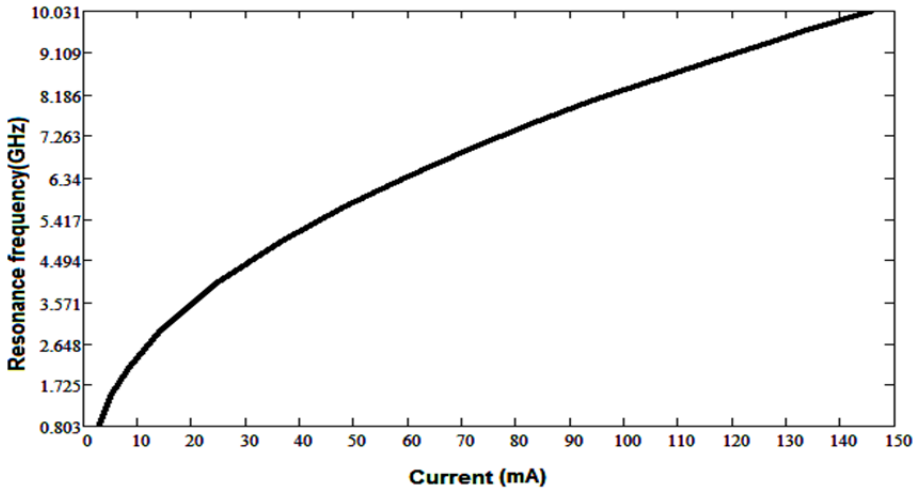

Figure (8) Resonance frequency of the modulation response versus the injection current.

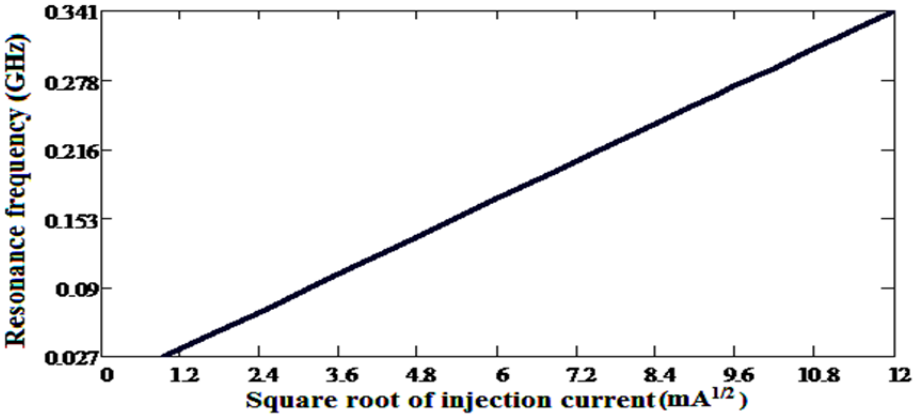

Figure (9) Resonance frequency versus the square root of the injection current.

Where the bias current values increase to 72 mA, 100 and 150 mA, the relaxation oscillation frequency increases dramatically and the (-3dB) bandwidth is significantly enlarged as shown in table (3) and Figure(10).

Table (3) Modulation response with injection current.

Current (mA)	Amplitude (dB)	BW (GHz)	OR frequency (GHz)	Efficiency GHz/(mA)$^{1/2}$
72	9	1.6	8.282	0.98
100	9.1	2	8.3	0.8366
150	8.4	3	10.18	0.8366

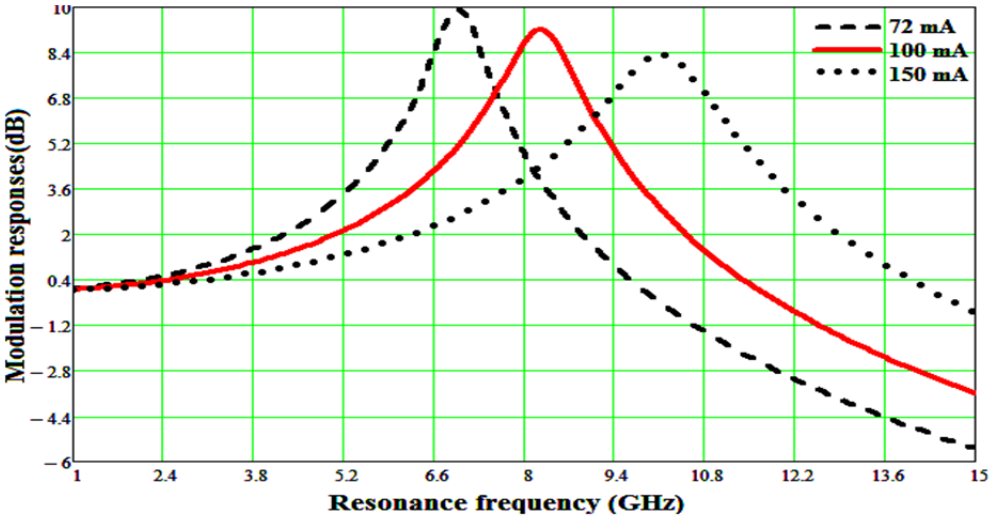

Figure (10) Modulation responses at several injected currents.

Maximum Bandwidth Of Quantum-Dot Lasers Diode

In fact the maximum modulation bandwidth of the QD lasers is mainly dependent on the QD carrier relaxation or capture times.

The MB (Modulation Bandwidth) which can be improved with decreasing carrier capture time. This is, the (-3 db) bandwidth is improved at first as increasing injected current, in addition, at large injected current, maximum value of the bandwidth is limited by *K* factor which is expressed as [9]:

$$f_{3\,dB\,max} = \sqrt{2}\frac{2\pi}{K} \quad \ldots (5)$$

That is the main contribution to bandwidth limitation of current QD lasers is due to three different effects, the *K*-factor is mainly determined by the photon lifetime and the effective capture time, the *K* factor can be minimized by choosing an optimum photon lifetime as shown in figure (11). One is to reduce the intrinsic capture time, where smaller *K* factor is obtained with a small intrinsic capture time of (*1 ps*) The maximum bandwidth limit is still as large as 30.16 GHz at photon lifetime is (*6.462 ps*) as shown in table (4) as shown in figure (12).

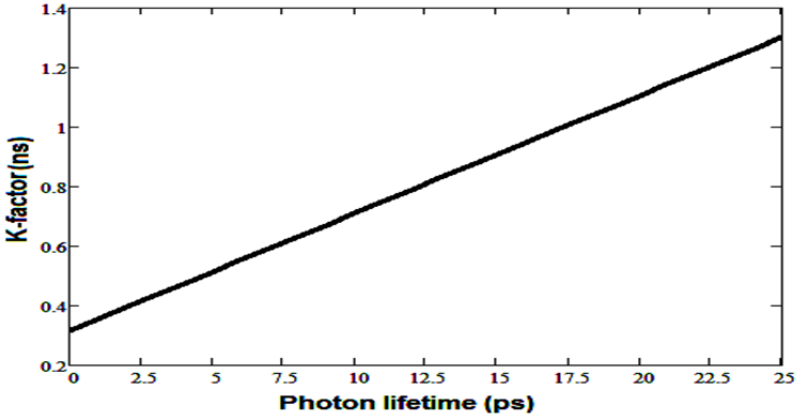

Figure(11) *K-factor* as a function of the optical lifetime.

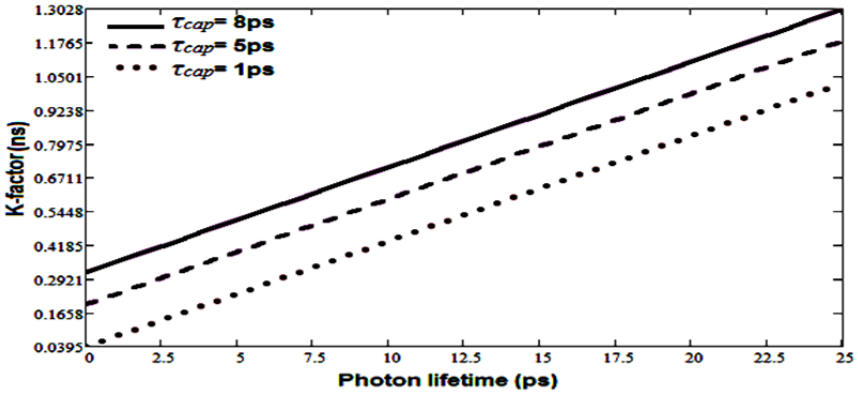

Figure (12) *K-facture* as a function of the lifetime at different value of the capture times.

Table(4) Effect of *capture time* on *K-factor* and the *maximum bandwidth* at *6.462ps* photon lifetime.

Capture time (ns)	K-factor (ns)	Maximum bandwidth (GHz)
1	29.46	30.16
5	45.25	19.6
8	57.09	15.56

Results

Power-current-voltage characteristics show that, the linear relation with small threshold current is 2mA, threshold current density is 25A/cm^2, for the output optical power range (0-10mW) under injection current of (2-60mA), and operating voltage is 0.92V and slope efficiency is 0.25W/A**.** Power spectra; optical output power of QD-LD is emitted over the wavelength range of (1298-1307nm) which approaches 1.3μm wavelength of optical communication systems. The highest relaxation oscillation frequency at room temperature is 10.18 GHz, corresponding to a modulation bandwidth of 3 GHz due to the small damping factor. Using these parameters, the maximum modulation bandwidth ($f_{-3dB}max$) is estimated as 15.56 GHz.

We can compare this theoretical model above results with one of the practical fabricated model of In(Ga)As/GaAs quantum-dot lasers with emission wavelength at 1295 nm at room temperature[13], the laser active region contains a three stack of QD layers with surface dot density of 4.56. 10^{10} cm^2. The result of fabricated model are threshold current density is 152.5 A/cm^2, the highest relaxation oscillation frequency measured is 1.8 GHz, corresponding to a modulation bandwidth of 2.8 GHz and the maximum modulation bandwidth (f-3db max) is 7.9 GHz [13].

CONCLUSION

Based on a four rate equation, an analytical modulation of QD lasers introduced. This numerical study explains of the ground state of the QD to the modulation response, finite carrier capture and relaxation times have been found to be physical limitations to the enhancement of the modulation bandwidth. As the photon density of the GS in the QD laser diode cavity increases by increasing the injected current, the relaxation oscillation frequency increases, which causes the increase in

modulation bandwidth. The -3dB bandwidth is improved at first as increasing the injected current. In addition, at large injected current, maximum value of the -3dB bandwidth is limited by *K*- factor, the *K*-factor is mainly determined by the photon lifetime and the effective capture time, the *K* -factor can be minimized by choosing an optimum photon lifetime**.** The results show that the QD laser has a small threshold current, suitable wavelength emitting and better frequency modulation characteristics.

RERFRANCES

[1] E. O. Chukwuocha and M.C Onyeaju, "Simulation of quantum dots (QDs) in the confinement regime", Ijaser Int., Journal of Applied Sciences and Engineering Research, Vol. 1, Issue 6, 2012.

[2] Dr.Khawla S. khashan,"Synthetic, Structural and Optical Properties of Cds Nanoparticles Prepared by Chemical Method", university of tech., Eng. & Tech. journal, Vol. 31, No.1, 2013.

[3] Dr. Azhar I. Hassan," A Theoretical Study of the Dynamical Behavior of SQW GaAs/AlGaAs Laser", university of tech., Eng. & Tech. journal, Vol. 28, No.20, 2010.

[4] P. Fei X, T. Yang, and H. M. Ji, "Temperature Dependent Modulation Characteristics for 1.3μm InAs/GaAs Quantum Dot Lasers", American Institute of Physics, Journal of Applied Physics 107, 2010.

[5] M. Gioannini and I. Montrosset, "Numerical Analysis of the Frequency Chirp in Quantum-Dot Semiconductor Lasers", IEEE, Journal of Quantum Electronics, Vol. 43, No. 10, October 2007.

[6] M. Gioannini, A. Sevega and I. Montrosset, "Simulations of Differential Gain and Linewidth Enhancement Factor of Quantum Dot Semiconductor Lasers", Springer, Journal of Optical and Quantum Electronics 38, pp. 381–394, 2006.

[7] H. Al-Husseini, A. H. Al-Khursan and S. Y. Al-Dabagh, "III-Nitride QD Lasers", Journal of the Open Nanoscience, Vol. 3, pp. 1-11, 2009.

[8] A. Fiore and A. Markus, "Differential Gain and Gain Compression in Quantum-Dot Lasers", IEEE, Journal of Quantum Electronics, Vol. 43, No. 3, March 2007.

[9] M. Ishida, N. Hatori, T. Akiyama and K. Otsubo, "Photon Lifetime Dependence of Modulation Efficiency and K Factor in 1.3μm Self-Assembled InAs/GaAs Quantum-Dot Lasers: Impact of Capture Time and Maximum Modal Gain on Modulation Bandwidth", American Institute of Physics, Applied Physics Letters, Vol. 85, No.18, 1 Nov. 2004.

[10] F. Grillot, B. Dagens, J. Provost, H. Su and L. F. Lester, "Gain Compression and above Threshold Linewidth Enhancement Factor in 1.3μm InAs–GaAs Quantum Dot Lasers", IEEE, Journal of Quantum Electronics, Vol. 44, No. 10, Oct. 2008.

[11] D. Pal, V. G. Stoleru, E. Towe and D. FIrsov, "Quantum Dot-Size Variation and Its Impact on Emission and Absorption Characteristics: an Experimental and Theoretical Modeling Investigation", the Japan Society of Applied Physics, Journal of Appl. Phys., Vol. 41, No. 2A, pp. 482–489, Feb. 2002.

[12] K. Iga, "Surface-Emitting Laser-Its Birth and Generation of New Optoelectronics Field", IEEE, Journal of Quantum Electronics, Vol. 6, No. 6, Nov. 2000.

[13] M . - H. MA, T. Y. WU and H. - H. L IN, " Relaxation oscillations and damping factors of 1.3 μm In(Ga)As/GaAs quantum-dot lasers", Optical and Quantum Electronics Vol. 36: pp. 927–933, 2004.